Simple empirical model for vibrational spectra of single-wall carbon nanotubes

Yu.N. Gartstein
Department of Physics, The University of Texas at Dallas,
P. O. Box 830688, FO23, Richardson, Texas 75083

A simple empirical model and approach are introduced for calculation of the vibrational spectra of arbitrary single wall carbon nanotubes. Differently from the frequently used force constants description, the model employs only invariant quantities such as variations of lengths and angles. All the salient qualitative features of vibrational spectra of nanotubes naturally follow from the vibrational Hamiltonian of graphene upon its isometric mapping onto a cylindrical surface and without any *ad hoc* corrections. A qualitative difference with previous results is found in a parabolic, rather than a linear, long wavelength dispersion of the transverse acoustic modes of the nanotubes. The parabolic dispersion is confirmed and elucidated in the provided continuum analysis of the vibrations. We also discuss and use an alternative definition of the nanotube unit cell with only two carbons per cell that illustrates a "true" longitudinal periodicity of the nanotubes, and of the corresponding Brillouin zone.

PACS numbers: 61.46.+w, 62.25.+g, 62.30.+d, 46.40.-f

I. INTRODUCTION

Vibrational spectra of individual single wall carbon nanotubes are of considerable interest and have been calculated previously within different frameworks such as an empirical force constant model,[1–3] *ab initio* studies[4] and tight-binding molecular dynamics.[5] It is known that the higher-frequency part of the nanotube spectra is relatively well represented already by the zone folding of the graphene spectrum. The lower-frequency part, however, has generic features owing to the one-dimensional character of nanotubes. Particularly, the spectra exhibit four types of acoustic modes with vanishing frequencies: one longitudinal, two transverse and one twisting. The existence of these modes has to do with general considerations – displacements of the tube as a whole along and perpendicular to its axis, and the rotation of the tube about the axis do not cost energy – rather than with specific nanotube interactions. Analogous vibrations were also discussed in the context of quantum wires as dilatational, flexural and torsional modes.[6] These modes are important contributors to the low-temperature quantized thermal conductance of such phonon waveguides.[7,8]

The frequently used force constant model of Ref. 1 was first developed for planar graphene based on the experimental data for graphite and then adapted for nanotube geometries. Direct application of the graphene force constant values was not found to lead to zero frequencies for all four modes mentioned above. To overcome this difficulty, special curvature corrections were introduced to the force constants.[1] In this paper we develop another empirical model, where the harmonic vibrational Hamiltonian of graphene is built using only "invariant" quantities such as variations of bond lengths, interbond and dihedral angles. Such a description is similar in spirit to used in conformational analysis and stereochemistry (see, e.g., Ref. 9) and in bond models for vibrations in covalent semiconductors (Ref. 10 and references therein). Further mapping of the graphene Hamiltonian onto a cylindrical surface of the nanotubes then allows to derive all features of arbitrary nanotube spectra "naturally", without any curvature corrections. This way the idea of Ref. 1 of using the same type of vibrational Hamiltonian for both graphene and nanotubes turns out to be realized with no need for *ad hoc* modifications.

We find a qualitative difference with the previously published results in a parabolic, rather than a linear, dispersion of the transverse acoustic modes of nanotubes. This parabolic dispersion is further illustrated in the corresponding continuum model of vibrations and is in agreement with the analysis of vibrations of elastic cylindrical shells.[11] The continuum model also shows the origin of another salient long wavelength feature of the nanotube spectra: a coupling of the longitudinal acoustic with the breathing mode. We believe the parabolic character of the low-frequency part of the transverse mode dispersion is quite generic similarly to the well-known bending waves of rods[12] with wavelengths much longer than the rod size. Such a parabolic dispersion was, e.g., calculated for the lowest flexural modes of quantum wires;[6,7] recent applications of elastic cylinder models also include vibrations of cytoskeletal filaments and microtubules.[13–15] To our knowledge, the parabolic dispersion was not calculated previously for carbon nanotubes.

With our approach we can easily calculate vibrational spectra of arbitrary (N, M) nanotubes. In doing this, we also employ an alternative definition of the nanotube unit cell with only two carbons per cell as opposed to possibly many carbon atoms of the conventional definition.[1] This way a "true" longitudinal periodicity of the nanotubes is elucidated. The period is a projection of one of the primitive vectors onto the nanotube axis, the primitive vector itself being in general not parallel to the axis. The Brillouin zones can correspondingly be wider than usually used and the total number of the vibrational branches turns out to be just $6d_c$, where d_c is the greatest common divisor of N and M.

Report Documentation Page

Form Approved
OMB No. 0704-0188

1. REPORT DATE	2. REPORT TYPE	3. DATES COVERED
10 FEB 2004	**N/A**	**-**

4. TITLE AND SUBTITLE	5a. CONTRACT NUMBER
Simple empirical model for vibrational spectra of single-wall carbon nanotubes	5b. GRANT NUMBER
	5c. PROGRAM ELEMENT NUMBER
6. AUTHOR(S)	5d. PROJECT NUMBER
	5e. TASK NUMBER
	5f. WORK UNIT NUMBER
7. PERFORMING ORGANIZATION NAME(S) AND ADDRESS(ES) **Department of Physics, The University of Texas at Dallas, P.O. Box 830688, FO23, Richardson, TX 75083, USA**	8. PERFORMING ORGANIZATION REPORT NUMBER
9. SPONSORING/MONITORING AGENCY NAME(S) AND ADDRESS(ES)	10. SPONSOR/MONITOR'S ACRONYM(S)
	11. SPONSOR/MONITOR'S REPORT NUMBER(S)

12. DISTRIBUTION/AVAILABILITY STATEMENT
Approved for public release, distribution unlimited

13. SUPPLEMENTARY NOTES
See also ADM001801.

14. ABSTRACT

15. SUBJECT TERMS

16. SECURITY CLASSIFICATION OF:			17. LIMITATION OF ABSTRACT	18. NUMBER OF PAGES	19a. NAME OF RESPONSIBLE PERSON
a. REPORT	b. ABSTRACT	c. THIS PAGE			
unclassified	**unclassified**	**unclassified**	**UU**	**10**	

For numerical computations, we will be using some parameterization of the model, specifically based on a set of data from Ref. 1 as well as on some experimental data. However, the numerical computations here serve mostly illustrative and qualitative purposes.

II. VIBRATIONAL HAMILTONIAN

Despite the fact that atoms of carbon nanotubes are arranged in a 3-d fashion, the excitations of nanotubes can be described in the way very similar to excitations of the planar graphene. To clearly see this connection for vibrational excitations, one can use local (position-dependent) coordinate systems for atomic displacements and the elastic potential energy written in an "invariant" form. This way the qualitative transformation from vibrational spectra of an infinite plane to spectra of curved cylindrical structures appear naturally without *ad hoc* corrections.

Following Ref. 1, we also consider carbon-carbon elastic interactions up to the fourth nearest neighbor. The harmonic potential energy $U = U_{\rm i} + U_{\rm o}$ is however expressed as a function of only invariant quantities such as variations of bond lengths and various angles. The first term $U_{\rm i}$ would correspond here to in-plane deformations of graphene and in general requires ten elastic parameters K_i^m:

$$\begin{aligned} U_{\rm i} &= \sum_{\langle ijk\rangle} \big[K_1(\delta l_{ij}^2 + \delta l_{jk}^2) + K_2 \delta\varphi_{ijk}^2 + K_3 \delta l_{ij}\delta l_{jk} \\ &+ K_4 \delta\varphi_{ijk}(\delta l_{ij} + \delta l_{jk})\big] \qquad (1a) \\ &+ \sum_{m=3}^{4} \sum_{\langle ijkl\rangle}^{\{il\}=m} [K_5^m \delta l_{ij}\delta l_{kl} + K_6^m \delta\varphi_{ijk}\delta\varphi_{jkl} \\ &+ K_7^m(\delta\varphi_{ijk}\delta l_{kl} + \delta\varphi_{jkl}\delta l_{ij})]\,, \qquad (1b) \end{aligned}$$

while term $U_{\rm o}$ would describe out-of-plane graphene distortions and needs three elastic parameters:

$$U_{\rm o} = \sum_{m=2}^{4} \sum_{\langle ijkl\rangle}^{\{il\}=m} K_8^m \delta\chi_{ijkl}^2. \qquad (2)$$

The structure of Eqs. (1,2) can be conveniently thought of in terms of triangular plaquettes $\langle ijk\rangle$ formed by bonds $\langle ij\rangle$ and $\langle jk\rangle$ connecting nearest carbons i and j, and j and k, respectively. Variation of bond $\langle ij\rangle$ length is denoted δl_{ij}, and variation of the inter-bond angle at the common carbon j denoted $\delta\varphi_{ijk}$. Correspondingly, Eq. (1a) completely describes the deformation energy of individual plaquettes. Equations (1b,2), on the other hand, completely describe the interactions of deformations on neighboring plaquettes; specifically, $\langle ijkl\rangle$ stands for plaquettes $\langle ijk\rangle$ and $\langle jkl\rangle$ that are adjacent along bond $\langle jk\rangle$. There are three different ways to form adjacent plaquette pairs and notation $\{il\} = m$ distinguishes them by indicating that carbons i and l are the mth nearest neighbors ($m = 2, 3, 4$), as illustrated in Fig. 1. (In case $m = 2$, it is actually plaquettes $\langle ijk\rangle$ and $\langle ljk\rangle$ that are adjacent along $\langle jk\rangle$. This case is not explicitly included in Eq. (1b) because of the constraint that a sum of inter-bond angles for three plaquettes surrounding a carbon atom is fixed.) The "out-of-plane" interaction, Eq. (2), involves the variations $\delta\chi_{ijkl}$ of the dihedral angles between corresponding plaquettes.

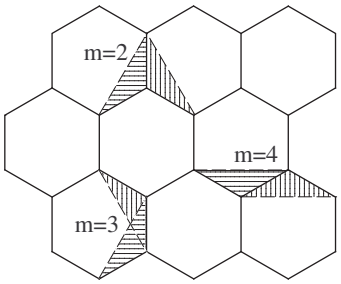

FIG. 1: Nomenclature of possible triangular plaquette pairs adjacent along a nearest-neighbor carbon-carbon bond. To guide the eye, individual adjacent plaquettes are filled with lines at different angles.

It is worth stressing that for the *planar* graphene, Eqs. (1,2) give the most general description of harmonic interactions involving up to the forth nearest neighbors. As such, it, of course, can reproduce a force constants description. The latter would be derived by expanding Eqs. (1,2) in the atomic pair differences. Evidently, then there would be certain relationships between a larger number of force constants as dictated by the invariance of the potential energy with respect to overall rotations.[16] Specifically, ten elastic parameters of Eq. (1) yield twelve force constants, comprising eight in-plane constants of the type explicitly considered in Ref. 1 and four constants mixing radial and tangential displacements that were implicitly set to zero in that reference. Three elastic parameters of Eq. (2) yield four out-of-plane force constants.[1]

The advantage of using invariant quantities in Eqs. (1,2) is that the same functional form of the potential energy can be directly used when carbon atom positions are (isometrically) mapped from the graphene plane onto the cylindrical surface of a nanotube. When on the nanotube surface, variations of the bond lengths and various angles just need to be calculated from the carbon atom displacements using the actual curved geometry. Of course, a new set of force constants appropriate for the now curved geometry can be again derived through the pair expansions. Force constants so obtained would automatically obey the correct relationships to satisfy the invariance with respect to rotations.

The standard translational invariance of the vibrational Hamiltonian is preserved if displacements of carbons are expressed not in terms of common (xyz) coordinates but in terms of local orthogonal coordinates (uvw): u - along the nanotube axis, v - perpendicular

to the tube axis and parallel to the tube surface, and w - perpendicular to the tube surface. These simple ideas are illustrated in more detail in Appendix A for an easier to follow example of the relationship between vibrations of a linear chain of atoms and vibrations of a ring of atoms. For the problem at hand, we use the local displacements $(u_{\mathbf{n}\alpha}, v_{\mathbf{n}\alpha}, w_{\mathbf{n}\alpha})$ depending on carbon $\mathbf{n}\alpha$ actual geometric position on the cylindrical surface of the tube. (Here carbon index $\mathbf{n}\alpha$ consists of a 2-d vector $\mathbf{n}$ specifying the unit cell of the parent graphene plane and $\alpha = 1, 2$ specifying one of the 2 carbons in the graphene unit cell.) With local displacement bases in place, the invariance of the vibrational Hamiltonian with respect to translations by graphene primitive vectors is held on equal footing in graphene and nanotubes: wave vectors $\mathbf{k}$ will "know" only differences between neighboring carbon indices $\mathbf{n}\alpha$. The problem is thereby reduced to calculation of the usual, "graphene-like", 6×6 dynamical matrix, but which naturally contains the correct mixing of the "in-plane" and "out-of-plane" displacements in nanotubes. Using proper quantization rules for the allowed phonon wavevectors, one can then readily derive the vibrational spectra of nanotubes of arbitrary chirality.

III. PRIMITIVE CELLS AND BRILLOUIN ZONES

The geometry of a single wall carbon nanotube is determined by the chiral vector[1]

$$\mathbf{C}_h = N\mathbf{a}_1 + M\mathbf{a}_2, \tag{3}$$

where $\mathbf{a}_1$ and $\mathbf{a}_2$ ($|\mathbf{a}_1| = |\mathbf{a}_2| = a$) are two primitive vectors of the 2-d graphene (hexagonal) crystal structure. Vector $\mathbf{C}_h$ is perpendicular to the nanotube axis. Conventionally,[1] the translational vector *parallel* to the tube axis is defined, which we denote here as $\mathbf{T}_D$: $\mathbf{T}_D = t_1\mathbf{a}_1 + t_2\mathbf{a}_2$, where $t_1 = (2M + N)/d_R$, $t_2 = -(2N + M)/d_R$ and d_R is the greatest common divisor of $(2N+M)$ and $(2M+N)$. The resulting unit cell of the nanotube built of $\mathbf{C}_h$ and $\mathbf{T}_D$ can contain many carbons $N_a = 4(N^2 + M^2 + NM)/d_R$, and the longitudinal period $|\mathbf{T}_D|$ of chiral tubes be much larger than a. The corresponding Brillouin zones (BZs) would then be narrow and contain many excitation spectrum (whether vibrational or electronic) branches.

In this paper we use an alternative picture of the unit cell and BZ construction that is aimed at having as small number of branches in the zone as possible. As described in more detail in Appendix B, this number of branches is determined by the greatest common divisor of N and M, denoted by d_c. The total number of continuous branches in BZ is equal to $2d_c$ per each degree of freedom of a carbon atom, that is, $6d_c$ for vibrational excitations. This corresponds to the nanotube unit cell containing *only two carbons* and which can, e.g., be built with primitive vectors $\mathbf{C}_h/d_c$ and $\mathbf{T}$. Different from vector $\mathbf{T}_D$, the translational vector $\mathbf{T} = P\mathbf{a}_1 + Q\mathbf{a}_2$ is in general *not parallel* to the nanotube axis. As discussed in Appendix B (see Eq. (B7)), integers P and Q here satisfy condition $MP - NQ = d_c$. It is the projection of vector $\mathbf{T}$ onto the axis that determines the longitudinal period

$$a_\parallel = \sqrt{3}d_c a^2/2C_h \tag{4}$$

and the width $2\pi/a_\parallel$ of the BZ.

The number of branches in the BZ is related to the transverse quantization of the 2-d wave vector $\mathbf{k}$ of the parent graphene band excitations:

$$\mathbf{k}\mathbf{C}_h = 2\pi l, \tag{5}$$

resulting in the appearance of one-dimensional sub-bands characterized by the integer quantum number l. The construction of the unit cell and BZ employed in this paper recognizes that there would be only d_c "unique" quantization levels (that is, only d_c independent integers l): all other allowed $\mathbf{k}$-vectors can be obtained with translations by graphene reciprocal vectors. Many branches of the conventional[1] BZ would not exhibit gaps at that BZ boundary; they would correspondingly become single continuous bands when properly "unfolded" in our construction. The quantization lines within our BZs can span several hexagons of the graphene reciprocal lattice (see example of Fig. 9).

IV. VIBRATIONAL SPECTRA

As was mentioned above, potential energy in Eqs. (1,2) is capable of reproducing results of the force constant model[1] for the graphene spectrum. Figure 2 (a), however, has been calculated with a parameterization of elastic constants K_i in Eqs. (1,2) such as to achieve only a close similarity to the published spectrum.[1] In our calculations, we chose to slightly and somewhat arbitrarily modify the tangential force constants $\phi_t^{(n)}$ from the published[1] values so as to satisfy $\phi_t^{(1)} + 6\phi_t^{(2)} + 4\phi_t^{(3)} + 14\phi_t^{(4)} = 0$. The latter equality is required by the rotational invariance – elastic energy should be zero for the overall rotation of the graphene plane. Original constants[1] do not obey it. A recently published new set of force constants[17] also does not satisfy this requirement. The overall scaling of elastic constants was chosen here so as to reproduce graphene experimental optical frequencies of 1580 and 868 cm^{-1}. Once the values of elastic constants K_i have been defined for graphene, the same values are used to calculate spectra of nanotubes, examples of which are shown in Figures 2 (b)–(d). As discussed in Sec. II, we do not need the knowledge of force constants of Ref. 1 for curved geometries because the Hamiltonian used automatically preserves all invariance requirements.

In displaying the nanotube spectra, we use the definition of BZ as discussed in Sec. III and Appendix B. With that definition, the BZ contains only $6d_c$ vibrational branches. For armchair tubes, $a_\parallel = a/2$ and the

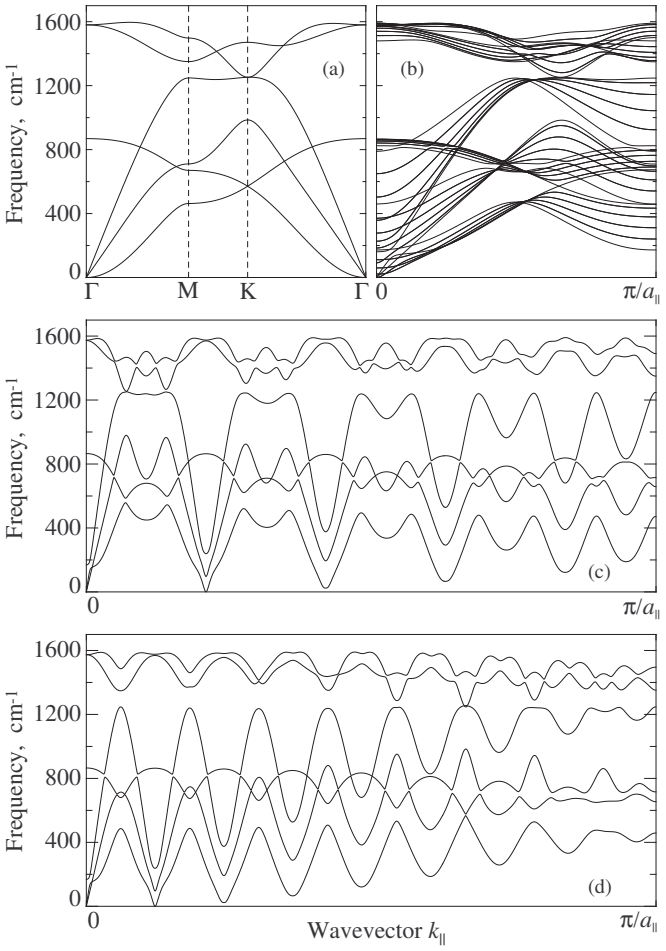

FIG. 2: Model vibrational spectra: (a) Graphene; (b) (10,10) tube; (c) (10,9) tube; (d) (16,1) tube. See text for definition of $a_\parallel$.

BZ in Figure 2 (b) is twice as wide as the conventional BZ, that picture would be restored by simple folding. Figure 2 (b) exhibits $d_c = 10$ "independent" transverse quantization levels. On the other hand, Figures 2 (c) and (d) with $d_c = 1$ correspond to only one transverse quantization level, that is, to six branches. Each polarization band/branch exhibits a continuous evolution of the polarization vectors with in general a strong $k_\parallel$ dependence. It is worth noting that transverse acoustic modes in this picture have their frequency vanishing at finite $k_\parallel$ (which, of course, lie in a hexagon of the graphene reciprocal lattice other than the one where $k_\parallel = 0$ is).

Figure 3 shows low-frequency parts of the vibrational spectra of the (10,10) and (10,0) tubes reduced to a single hexagon of the reciprocal lattice. Panel (a) can be directly compared to the published results[2] derived from the model of Ref. 1. Apart from the small differences, such as values of acoustic velocities, likely caused by our modification of the force constants, there is one qualitative disparity. The dispersion of the transverse acoustic modes in Figure 3 is clearly seen to be parabolic in contrast to a linear dispersion discussed in Refs. 1,2,5. The parabolic dispersion is seen over a wider range of $k_\parallel$ on going to tubes of smaller radii, compare Figures 3 (a) and (b). In Sec. V we give an analytic confirmation of this observation within a framework of a continuum mechanics.

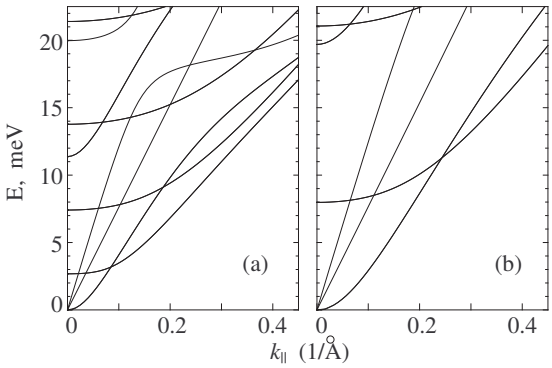

FIG. 3: The low-frequency part of calculated nanotube vibrational spectra: (a) (10,10) tube, (b) (10,0) tube. Note that here wave vectors $k_\parallel$ are measured with respect to closest Γ points of hexagons of the reciprocal graphene lattice.

V. CONTINUUM ANALYSIS

Analysis of deformations and vibrations of thin-walled elastic cylinders goes back as far as to Rayleigh and Love; see, e.g., Refs. 18–21, references therein, and Refs. 11,22 for a dedicated analysis of vibrations.

In the case of a planar, graphene, structure, the continuum potential elastic energy can be written as

$$U_{\rm i} = \frac{\rho}{2}\int dx\,dy\,\left[C_1(u_x+v_y)^2 + C_2\left((u_y+v_x)^2-4u_xv_y\right)\right], \quad (6)$$

$$U_{\rm o} = \frac{\rho}{2}\int dx\,dy\,\left[D_1(w_{xx}+w_{yy})^2 + D_2(w_{xy}^2-w_{xx}w_{yy})\right]. \quad (7)$$

Here x is a coordinate that would later become along the cylinder axis and y coordinate along the cylinder circumference, ρ is the mass density. Displacements fields u, v and w would become, respectively, parallel to the cylinder axis, parallel to its circumference, and perpendicular to the cylindrical surface; x and y subindices denote the differentiation over corresponding coordinates. This type of deformation energy is well known in the continuum mechanics of plates[12,20] and can be readily derived from the discrete form (1,2). In the former picture, elastic constants C_1, C_2, D_1 and D_2 in Eqs. (6,7) are expressed in terms of stretching and bending rigidities and Poisson's ratio. In the latter derivation, they would be expressed through constants K's in Eqs. (1,2). Note, however, that

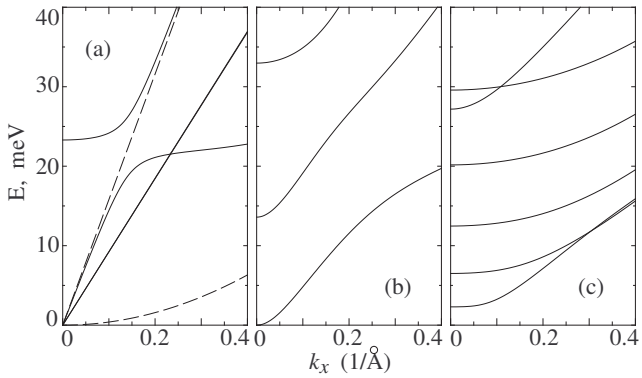

FIG. 4: Branches of the vibrational spectra obtained in the continuum model described in the text at (a) $k_y = 0$, (b) $k_y = 1/R$, (c) $k_y = n/R$ with $n \geq 2$. Calculations were performed for $R = 6.78$ Å that one would have for the (10,10) tube. Elastic parameters used in calculations for this Figure would correspond to graphene velocities $c_{la} = 24$ km/s, $c_{ta} = 14$ km/s. Dispersion of the out-of-plane graphene vibrations $\omega = \delta k^2$ was taken with $\delta = 6 \times 10^{-7}$ m^2/s (see Ref. 4), and $D_2/D_1 = 4C_2/C_1$. Graphene results are shown by the dashed lines for comparison. Dispersion of the graphene transverse acoustic mode practically coincides with that of the nanotube twisting mode.

Eqs. (1,2) should then be transformed only in the context of purely acoustic deformations, in which two carbons in a hexagon move "in-phase". That is why we will be dealing here with the 3×3 matrix in Eq. (9) rather than with a 6×6 dynamical matrix. One can develop a continuum model that would include optical "out-of-phase" deformations as well. The deformation energy of type of Eqs. (6,7) was already proved to be useful in studies of large deformations of carbon nanotubes.[23]

The modification of Eqs. (6,7) upon formation of a cylindrical body in continuum mechanics is, e.g., discussed in Refs. 11,20,21. As is also shown in Appendix A for a discrete model, this corresponds to a simple substitution in (6,7): $v_y \to v_y + w/R$ and $w_y \to w_y - v/R$, R being the cylinder radius. Using this substitution, one can easily study the problem of small vibrations of a continuum cylinder. The vibrational frequencies ω for the plane waves with a two-dimensional wave vector (k_x, k_y) are determined from the eigenvalue equation

$$\omega^2 \mathbf{d} = \mathbf{M}\mathbf{d}, \tag{8}$$

where displacement vector $\mathbf{d} = (u, v, w)$ and matrix $\mathbf{M}(k_x, k_y)$ is

$$\mathbf{M} = \begin{bmatrix} C_1 k_x^2 + C_2 k_y^2 & (C_1 - C_2) k_x k_y & iAk_x/R \\ (C_1 - C_2) k_x k_y & \tilde{C}_1 k_y^2 + \tilde{C}_2 k_x^2 & -iBk_y/R \\ -iAk_x/R & iBk_y/R & \omega_b^2 + D_1 (k_x^2 + k_y^2)^2 \end{bmatrix}. \tag{9}$$

Here $\tilde{C}_1 = C_1 + D_1/R^2$, $\tilde{C}_2 = C_2 + D_2/R^2$, $A = 2C_2 - C_1$, $B = C_1 + (D_1 + D_2/2)k_x^2 + D_1 k_y^2$ and $\omega_b^2 = C_1/R^2$.

In the case of the planar structure, $R \to \infty$, Eqs. (8,9) lead to two acoustic waves of in-plane vibrations (with longitudinal $c_{la} = C_1^{1/2}$ and transverse $c_{ta} = C_2^{1/2}$ velocities) and an acoustic wave of the out-of-plane vibrations with a parabolic spectrum $\omega = D_1^{1/2}(k_x^2 + k_y^2)$, see Figure 4 (a).

For a cylinder/tube of a finite radius R, the transverse quantization imposes a restriction on values of $k_y = n/R$, where n is an integer. Of special interest to us here are values of k_y equal to 0 and to $\pm 1/R$. The case of $k_y = 0$ (Fig. 4 (a)) yields two of the four acoustic modes of the tube with vanishing frequencies: (i) the longitudinal mode with a low-frequency dispersion coinciding with the longitudinal acoustic wave of the graphene and (ii) the twisting mode whose dispersion is somewhat modified from the transverse acoustic mode of graphene by virtue of the elastic constant D_2: $c_{ta} = \tilde{C}_2^{1/2}$. The longitudinal mode in the case of the cylinder couples with the breathing mode, whose frequency at $k_x = 0$ is ω_b and whose dispersion is determined by constant D_1. As a result of this coupling, an anti-crossing behavior of the branches arises as is clearly seen in the Figure. (iii) The two other, degenerate, acoustic modes of the tube spectrum, usually referred to as transverse acoustic modes for carbon nanotubes[1] or as flexural modes in other applications,[6,13,14,22] correspond to $k_y = \pm 1/R$ (Fig. 4 (b)). It is apparent from the Figure that these modes have a parabolic spectrum. In fact, one can easily show this analytically by the perturbation analysis of (8,9) in k_x: contributions to the linear coefficient in dispersion $\omega(k_x)$ exactly cancel. The low-frequency parabolic dispersion of these modes, although modified by the curvature rigidity, Eq. (7), is mainly determined by the in-plane stretching rigidity, Eq. (6). Neglecting Eq. (7), one would obtain the long wavelength, for $k_x R \ll 1$, dispersion of this mode as $\omega(k_x) = (2(C_1 - C_2)C_2/C_1)^{1/2} k_x^2 R$. Evidently, the parabolic character of the dispersion becomes even more apparent for smaller-radius tubes. These modes correspond to bending vibrations of the tube as a whole and, in this sense, are similar to the bending vibrations of rods, whose generic long-wavelength parabolic dispersion is well known.[12] Similarities between Figures 4 and 3 (a) are obvious. Note, however, some quantitative differences caused by different values of effective parameters.

VI. SUMMARY AND DISCUSSION

We have described a simple empirical model, in which vibrations of the graphene and individual single wall carbon nanotubes are treated and calculated on the same footing. Differently from the force constant model, our model uses only "invariant" quantities: variations of bond lengths, interbond and dihedral angles. As a result, the isometric mapping from the planar graphene onto a cylindrical surface of nanotubes automatically preserves all the right relationships between equivalent force constants. Importantly, all calculated vibrational spectra of

nanotubes correctly exhibit four types of acoustic excitations with vanishing frequencies (one longitudinal, two transverse and one twisting), which are derived naturally and follow from the symmetries of the underlying system. Although the results obtained are largely similar to the earlier published, we have also found an important qualitative difference. The long-wavelength dispersion of the transverse acoustic modes is shown to be parabolic rather than linear. One consequence of this is that the vibrational density of states should exhibit a one-dimensional singularity near zero frequency. We cannot exclude that there can be other physical implications of our finding, although this apparently is not the case for the quantized ballistic thermal conductance,[7,8] for which the exact dispersion law is irrelevant. These long-wavelength (wavelength much larger than the tube radius) transverse modes correspond to bending oscillations of a nanotube as a whole and, therefore, are similar to bending vibrations of rods, whose low-frequency spectrum is known to be parabolic.[12] The parabolic dispersion is, e.g., evident in calculations of the lowest flexural modes of quantum wires.[6,7] The origin of the parabolic dependence for nanotubes has been analytically illustrated using a continuum elastic model similar to used in the analysis of vibrations of cylindrical shells.[11] The continuum model also clarified the coupling between longitudinal acoustic and breathing modes resulting in the anti-crossing behavior clearly seen in the calculated spectra of nanotubes.

The simplicity of our model allows us to easily calculate vibrational spectra of nanotubes of arbitrary chiralities. To better handle such spectra, we employed an alternative definition of the nanotube unit cell with only two carbons per cell. This definition reveals a "true" longitudinal periodicity of carbon nanotubes that can be substantially shorter than used in the conventional definition.[1]

Being a result of the straightforward isometric mapping, the model presented in this paper, has its qualitative limitations. For instance, it does not automatically yield the curvature-induced softening of the phonon modes observed in *ab initio* studies such as that of the twisting mode,[4] or more complex dependencies for the breathing mode.[4,24] Of course, these effects are not deducible from the graphene properties. To describe them, the model would need to include both the relaxation of nanotube geometries (mapping would not be exactly isometric) as well as an explicit dependence of the elastic energy on nanotube radius and with the axial anisotropy.[27] We discussed such a generalization in the context of uniform deformations,[25] which, e.g., leads to the chirality-dependent stiffness of nanotubes.[26] We believe the present model can also be further developed in this regard and correspondingly parameterized by comparison with *ab initio* calculations. A more accurate parameterization is, needless to say, required even for the present model. Such quantitative aspects have not been pursued in this paper.

Acknowledgments

This work was started in the context of DARPA program on "Phonon Engineering" funded under the contract No. MDA 972-02-C-0044. I am grateful to V. Agranovich, R. Baughman, A. Efros, M. Kertesz and A. Zakhidov for discussions and various inputs related to the subject.

APPENDIX A: A RING EXAMPLE

Here we study in more detail a simpler illustrative example of the relationship of vibrations of an infinite linear atomic chain and a ring of atoms. For clarity, displacements of atoms are restricted to the plane in which a ring and chain belong. Atom-atom interactions correspond to formation of bonds and result both in stretching and bending rigidity of a linear chain. Figure 5 is a picture of the ring consisting of $N = 10$ atoms, which is assumed to preserve the nature of interactions in the chain. The figure shows a common system of coordinates (y, z) as well as local systems (v, w) related to the tangential and normal displacements of the corresponding atom. Obviously, the kinetic energy

$$T = \frac{M}{2}\sum_n (\dot{y}_n^2 + \dot{z}_n^2) = \frac{M}{2}\sum_n (\dot{v}_n^2 + \dot{w}_n^2), \qquad \text{(A1)}$$

where n is the 1-d positional index of the atom along the ring circumference. We first write the potential energy of a linear chain in an invariant form as

$$U = \frac{K}{2}\sum_n \delta l_n^2 + \frac{K_b l^2}{2}\sum_n \delta\chi_n^2, \qquad \text{(A2)}$$

where the first term describes the stretching and second the bending rigidity. Then we assume that the same functional form holds for the ring. From the geometry of

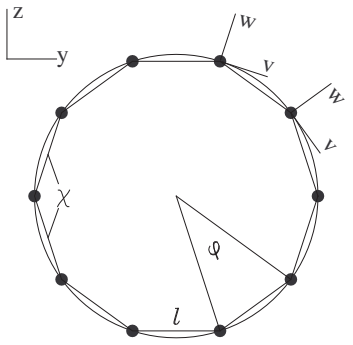

FIG. 5: A ring of $N = 10$ atoms connected by interatomic "bonds" (thicker lines). The stretching rigidity corresponds to variations of the bond lengths l, the bending rigidity to variations of the inter-bond angles χ. Number of atoms N (or the radius of the ring) determines the angle $\varphi = 2\pi/N$.

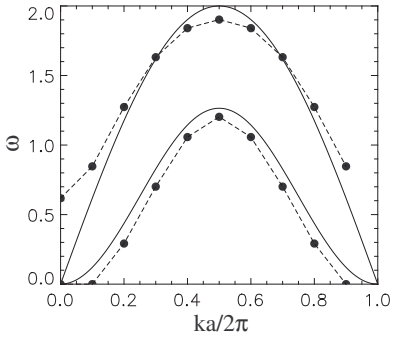

FIG. 6: The vibrational spectra of the linear chain (solid lines) and of the ring (filled circles) of atoms. The parameters used for the plot are $K/M = 1$ and $K_b/M = 0.1$.

Figure 5, the variation of the bond lengths, as a function of the local displacements, is

$$\delta l_n = (v_{n+1} - v_n)\cos(\varphi/2) + (w_{n+1} + w_n)\sin(\varphi/2), \quad \text{(A3)}$$

while the variation of the inter-bond angles

$$\begin{aligned} l \cdot \delta\chi_n &= (2w_n - w_{n+1} - w_{n-1})\cos(\varphi/2) \\ &+ (v_{n+1} - v_{n-1})\sin(\varphi/2). \end{aligned} \quad \text{(A4)}$$

For the linear chain ($\varphi = 0$ and $v_n = y_n$, $w_n = z_n$), Eq. (A3) describes a conventional longitudinal stretching while Eq. (A4) would yield a conventional local curvature. Tangential and normal vibrations in a linear chain are fully decoupled. The corresponding two branches of the vibrational spectrum are simply

$$\begin{aligned} \omega_s^2(k) &= (4K/M)\sin^2(ka/2), \\ \omega_b^2(k) &= (16K_b/M)\sin^4(ka/2), \end{aligned} \quad \text{(A5)}$$

where $a = l$ is the distance between the atoms along the chain. This spectrum is shown in Figure 6 with solid lines.

In the curved system (our ring with $\varphi \neq 0$), on the other hand, tangential and normal displacements *are* coupled, as is well known in the elasticity theory for curved surfaces[12,20] and clearly seen in Eqs. (A3,A4). If we were to use the common system of coordinates for displacements (y_n, z_n), the atom contributions to the potential energy, Eq. (A2), would be position dependent and the translational invariance with respect to $n \to n + 1$ would be lost. With the local coordinates (v_n, w_n), this invariance is preserved and one can directly use the conventional transition to $k-$states, which would now be quantized as

$$k = (2\pi/Na)i, \quad i = 0, \ldots N - 1. \quad \text{(A6)}$$

The unit cell length $a > l$ here is now the distance between the atoms of the ring along its circumference. The derivation of the spectrum from the equations of motion follows straightforwardly from Eqs. (A1–A4), and the results are shown in Figure 6 with filled circles. In accordance with Eq. (A6), it is now a set of discrete frequencies. The coupling between normal and tangential displacements resulted in important qualitative modifications of the spectrum, which have been obtained exactly and naturally. Particularly, one notices 3 zero-frequency modes. Two of them (with $i = 1$ and $i = N - 1$, or $i = -1$, in Eq. (A6) – precisely one wavelength on the ring circumference) correspond to the displacements of the ring as a whole in two orthogonal directions. The other (with $i = 0$) is a pure tangential mode describing the rotation of the ring as a whole. The $k = 0$ finite-frequency mode, on the other hand, is a pure normal, breathing, mode that "borrowed" its strength from the parent stretching oscillations of the linear chain.

Equations (A3,A4) can be used to study the continuum limit, when, keeping the same radius R, we increase the number of atoms $N \to \infty$ and bond length $l \to 0$. Then, evidently,

$$\begin{aligned} \delta l/l &\to [\partial v/\partial y + w/R], \\ \delta\chi/l &\to -\partial\left[\partial w/\partial y - v/R\right]/\partial y. \end{aligned} \quad \text{(A7)}$$

The expressions in brackets in Eq. (A7) provide a recipe for a transition from the continuum model of a chain to the continuum model of a ring. The subsequent analysis of vibrations is straightforward with the wavevector k quantized as $kR = n$ (n being an integer) yielding three zero-frequency modes and the breathing mode as in the discrete case above.

It should be noted here that in reality the very values of the unit cell length a and elastic constants K, K_b can in fact somewhat differ for the ring and the linear chain, and the difference would be $N-$dependent as determined by the equilibrium bond length in the ring. In this sense, what is compared in Figure 6 is the structure of the spectra for the same values of the essential parameters upon isometric mapping of the linear system onto a circular ring. In addition, the elastic energy of the ring could in general contain terms absent in the energy of the chain, such as $\delta\chi_n\delta l_n$. They are not deducible from the functional form of the linear system and would have to be explored on their own. We also note that Eq. (A2) can be generalized to include longer range interactions.

APPENDIX B: TRANSVERSE QUANTIZATION AND UNIT CELLS

Two carbons connected by $\mathbf{C}_h$ (Eq. (3)) on the graphene plane correspond to the same carbon on the nanotube after wrapping. The effective 2-d cyclic condition can therefore be written as

$$\mathbf{R}_{nm} + \mathbf{C}_h = \mathbf{R}_{nm}, \quad \mathbf{R}_{nm} = n\mathbf{a}_1 + m\mathbf{a}_2, \quad \text{(B1)}$$

$\mathbf{R}_{nm}$ being the position of one of the carbons (there are two of them) of an arbitrary unit cell of graphene. If $\mathbf{k}$

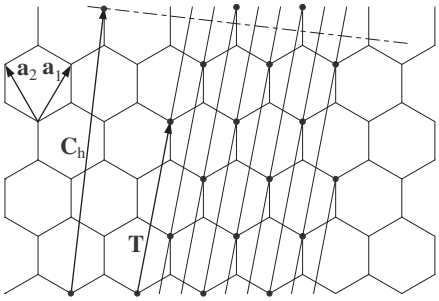

FIG. 7: Unwrapped (3,2) tube with carbons rearranged to form a horizontal strip here. The tube axis is shown by the dash-dotted line. Here $d_c = 1$ and the $\mathbf{T}$ vector, Eq. (B2), is defined by the (P, Q) pair (2,1). Small circles connected by thinner lines indicate a sequence of carbons reached by the $\mathbf{T}-$translation. It is transparent that all hexagons of the strip would be visited this way, forming an effectively 1-d enumeration of Eq. (B5). The conventional vector $\mathbf{T}_D = 7\mathbf{a}_1 - 8\mathbf{a}_2$ and such a unit cell would have 38 hexagons.

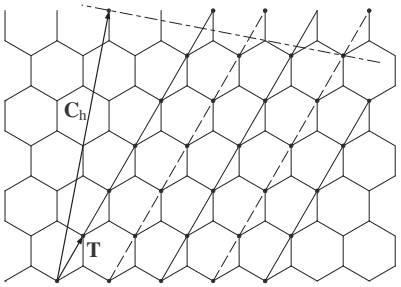

FIG. 8: Unwrapped (4,2) tube with carbons rearranged to form a horizontal strip here. The tube axis is shown by the dash-dotted line. Here $d_c = 2$ and the $\mathbf{T}$ vector, Eq. (B2), is defined by the "reduced" (P, Q) pair (1,0). Two sequences of carbons resulting from $\mathbf{T}-$translations are shown by thinner lines: small circles of one sequence are connected by the solid line, and circles of the other by the dashed line. Translation from one sequence to the other is achieved with vector $\mathbf{C}_h/2$. All hexagons of the strip would be visited this way, forming effective enumeration of Eq. (B8). The conventional vector $\mathbf{T}_D = 4\mathbf{a}_1 - 5\mathbf{a}_2$ and such a unit cell would have 28 hexagons.

is the 2-d wave vector of the band excitations, then in the infinite graphene plane it would have two independent continuous components. In nanotubes, the cyclic condition leads to the transverse quantization of Eq. (5). In other words, wave vectors $\mathbf{k} = \mathbf{k}_\perp + \mathbf{k}_\parallel$ allowed by Eq. (5) lie only on certain quantization lines in the reciprocal plane of graphene, $\mathbf{k}_\perp$ being quantized according to Eq. (5) and $\mathbf{k}_\parallel$ being actually a 1-d continuous wave vector parallel to the tube axis.

Let us define vector

$$\mathbf{T} = P\mathbf{a}_1 + Q\mathbf{a}_2 \tag{B2}$$

with integer P and Q. From Eqs. (3) and (B2), one finds

$$\mathbf{a}_1 = (-Q\mathbf{C}_h + M\mathbf{T})/\Delta, \quad \mathbf{a}_2 = (P\mathbf{C}_h - N\mathbf{T})/\Delta, \tag{B3}$$

where

$$\Delta = MP - NQ. \tag{B4}$$

Evidently, *if* one can find such P and Q (of course, we are interested in the "smallest" P and Q) for a given tube (N, M) that $\Delta = \pm 1$ in Eq. (B4), then original primitive vectors $\mathbf{a}_1$ and $\mathbf{a}_2$ in Eq. (B3) will be represented through integer amounts of $\mathbf{C}_h$ and $\mathbf{T}$. Correspondingly, an arbitrary vector $\mathbf{R}_{nm}$, Eq. (B1), will be expressed through integer quantities of $\mathbf{C}_h$ and $\mathbf{T}$ as well. Since the cyclic condition defines $\mathbf{R}_{nm}$ in Eq. (B1) with accuracy to $\mathbf{C}_h$, this would actually mean that the position of any hexagon in the unwrapped tube is determined through a single vector $\mathbf{T}$:

$$\mathbf{R}_{nm} \to \mathbf{R}_i = i\mathbf{T}, \tag{B5}$$

where, e.g., $i = nM - mN$ for $\Delta = 1$. One can think of the corresponding unit cell built of $\mathbf{C}_h$ and $\mathbf{T}$ that would contain only 2 carbons in the cell. Of course, vector $\mathbf{T}$ *does not have to be parallel* to the tube axis. The projection of $\mathbf{T}$ on the nanotube axis $T_\parallel = \sqrt{3}a^2\Delta/2C_h$ – it would be directed in opposite ways for $\Delta = 1$ vs $\Delta = -1$ – and its modulus determines the corresponding longitudinal period

$$a_\parallel = \sqrt{3}a^2/2C_h, \tag{B6}$$

where $C_h = |\mathbf{C}_h|$. Note that vector $\mathbf{T}$ is different from the symmetry vector defined in Ref. 1.

It is easy to see that the picture described in the previous paragraph is indeed realized whenever $d_c = 1$ – we will call it the irreducible case – where d_c is the greatest common divisor of N and M. (Considering only positive N and M does not restrict the generality.) Then, in fact, any integer value of Δ in Eq. (B4) can be established with an appropriate choice of P and Q. Examples of positive (P, Q) pairs satisfying $\Delta = 1$ are listed here as $(N, M) \to (P, Q)$: $(3, 1) \to (1, 0)$, $(3, 2) \to (2, 1)$, $(5, 2) \to (3, 1)$, and $(10, 9) \to (9, 8)$. An illustration for the (3,2) tube is shown in Figure 7. A visual picture of the irreducible case is that of a 1-d chain (of period $|\mathbf{T}|$) that is wrapped around the nanotube cylinder with an appropriate helix angle, as is clearly seen from Figure 7.

"Reducible" cases – with $d_c > 1$ – can be described in a similar but somewhat more involved fashion. One would extract the irreducible structure factors N_1 and M_1:

$$N = d_c N_1, \quad M = d_c M_1,$$

so that the greatest common divisor of N_1 and M_1 equals 1. Then the procedure described above for the irreducible case can be applied for the geometry (N_1, M_1) resulting in the first translational vector $\mathbf{T}$. In other words, integers P and Q of Eq. (B2) should satisfy condition

$$MP - NQ = d_c. \tag{B7}$$

One however could not visit all hexagons by using only so defined $\mathbf{T}$. The needed second translational vector

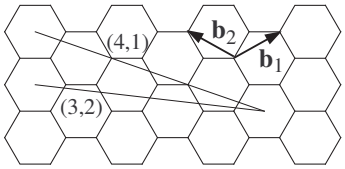

FIG. 9: An illustration of the range of variation of $\mathbf{k}_\parallel$ for (3,2) and (4,1) tubes. In the former case $\mathbf{K}_2 = 2\mathbf{b}_1 - 3\mathbf{b}_2$, in the latter case $\mathbf{K}_2 = \mathbf{b}_1 - 4\mathbf{b}_2$. The corresponding ranges are shown as thick lines between the centers of hexagons of the reciprocal lattice of graphene. Each line crosses several hexagons. If all inside-a-hexagon segments are displaced to one hexagon with a graphene reciprocal vector, they would form a traditional picture of quantization lines in the first BZ of graphene.

can be found as $\mathbf{C}_h/d_c$. The resulting enumeration of all hexagons will then read as

$$\mathbf{R}_{nm} \to \mathbf{R}_{ij} = i\mathbf{T} + j\mathbf{C}_h/d_c, \quad j = 0, 1, \dots d_c - 1. \quad \text{(B8)}$$

Index i here is, as in Eq. (B5), an arbitrary integer that would define unique carbons while j results only in d_c unique translations due to the cyclic condition in Eq. (B1). An illustration for the (4,2) tube is shown in Figure 8. A visual picture of the irreducible case is then of d_c 1-d chains (of period $|\mathbf{T}|$) that are wrapped around the nanotube cylinder with an appropriate helix angle. The elementary unit cell contains two carbons and built of vectors $\mathbf{T}$ and $\mathbf{C}_h/d_c$. Longitudinal periodicity will again be determined by the projection of vector $\mathbf{T}$ on the nanotube axis which is Eq. (4) becoming Eq. (B6) at $d_c = 1$.

For the reciprocal lattice vectors, defined through $\mathbf{K}_1 \cdot \mathbf{C}_h = 2\pi$, $\mathbf{K}_2 \cdot \mathbf{T} = 2\pi$, $\mathbf{K}_1 \cdot \mathbf{T} = 0$, and $\mathbf{K}_2 \cdot \mathbf{C}_h = 0$, one readily obtains

$$\mathbf{K}_1 = -Q\mathbf{b}_1 + P\mathbf{b}_2, \quad \mathbf{K}_2 = M_1\mathbf{b}_1 - N_1\mathbf{b}_2,$$

where $\mathbf{b}_1$ and $\mathbf{b}_2$ are primitive graphene reciprocal vectors defined with respect to $\mathbf{a}_1$ and $\mathbf{a}_2$. One easily finds that $|\mathbf{K}_2|$ indeed coincides with $2\pi/a_\parallel$. An illustration for cases of (3,2) and (4,1) tubes is given in Figure 9.

This way one arrives at the band excitation picture with $2d_c$ (for each component of the wave function or polarization) continuous bands corresponding to 2 atoms in the unit cell and d_c transverse quantization levels, e.g. with quantum numbers

$$l = -d_c/2 + 1, \dots, 0, \dots d_c/2. \quad \text{(B9)}$$

The latter define the quantized component of the parent 2-d quasi-momentum $\mathbf{k}$ perpendicular to the tube axis:

$$k_\perp = (2\pi/C_h)l. \quad \text{(B10)}$$

The continuous component $k_\parallel$ parallel to the tube axis, on the other hand, would be defined within a BZ whose width is

$$2\pi/a_\parallel = 4\pi C_h/\sqrt{3}d_c a^2. \quad \text{(B11)}$$

One can easily calculate that the resulted number of continuous bands and the width of the BZ lead to the correct total number of states in the system, which corresponds to $2C_h/\sqrt{3}a^2$ hexagons per unit length of the nanotube.

The conclusion that there are only d_c "truly unique" quantization levels can be confirmed another way as well. If $\mathbf{G} = n_1\mathbf{b}_1 + n_2\mathbf{b}_2$ is the vector of the reciprocal lattice of graphene, then $\mathbf{k}_1 = \mathbf{k} + \mathbf{G}$ is physically equivalent to $\mathbf{k}$. In general, $\mathbf{k}$ and $\mathbf{k}_1$ may correspond to different quantum numbers in Eq. (5), say l and l_1. One derives the integer difference of these quantum numbers as

$$\delta l = l - l_1 = n_1 N + n_2 M = d_c(n_1 N_1 + n_2 M_1). \quad \text{(B12)}$$

Once again, the last, "irreducible", factor in Eq. (B12) can take any integer values:

$$n_1 N_1 + n_2 M_1 = 0, \pm 1, \pm 2, \dots,$$

with appropriate choices for integer n_1 and n_2. It is then clear that the number of unique sub-bands in the extended scheme equals precisely d_c – one can, e.g., choose quantum numbers of Eq. (B9) for "independent" sub-band indexing, all other values of l would be reducible to independent values with the appropriate adjustment for the one-dimensional continuous quasi-momentum $k_\parallel$.

It is worth mentioning that in the (N, M) family of nanotubes with $N > M$, it is the armchair and zigzag nanotubes that have maximal number of transverse quantization levels $d_c = N$. The tubes immediately next to them, $(N, N-1)$ and $(N, 1)$, on the other hand, would have only one quantization level. The armchair tubes have then the longitudinal period of $a/2$, twice as small as is with the conventional definition.[1] One can easily see it with $\mathbf{T}$ vector defined by the (P, Q) pair (1,0).

[1] R. Saito, G. Dresselhaus, and M. S. Dresselhaus, *Physical Properties of Carbon Nanotubes* (Imperial College Press, London, 1998).

[2] M. S. Dresselhaus and P. Eklund, Adv. Phys. **49**, 705 (2000).

[3] J. X. Cao, X. H. Yan, Y. Xiao, Y. Tang, and J. W. Ding, Phys. Rev. B **67**, 045413 (2003).

[4] D. Sánchez-Portal, E. Artacho, J. M. Soler, A. Rubio, and P. Ordejón, Phys. Rev. B **59**, 12678 (1999).

[5] J. Yu, R. K. Kalia, and P. Vashishta, J. Chem. Phys. **103**,

6697 (1995).
[6] N. Nishiguchi, Y. Ando, and M. N. Wybourne, J. Phys.: Condens. Matter **9**, 5751 (1997).
[7] L. G. C. Rego and G. Kirczenow, Phys. Rev. Lett. **81**, 232 (1998).
[8] K. Schwab, E. A. Henriksen, J. M. Worlock, and M. L. Roukes, Nature **404**, 974 (2000).
[9] E. L. Eliel, S. H. Wilen, and M. P. Doyle, *Basic Organic Stereochemistry* (Wiley, New York, 2001).
[10] P. Y. Yu and M. Cardona, *Fundamentals of Semiconductors* (Springer, Berlin, 1999).
[11] Š. Markuš, *The Mechanics of Vibrations of Cylindrical Shells* (Elsevier, Amsterdam, 1988).
[12] L. D. Landau and E. M. Lifshitz, *Elasticity Theory* (Pergamon, Oxford, 1986).
[13] Y. M. Sirenko, M. A. Stroscio, and K. W. Kim, Phys. Rev. E **53**, 1003 (1996).
[14] Y. M. Sirenko, M. A. Stroscio, and K. W. Kim, Phys. Rev. E **54**, 1816 (1996).
[15] M. A. Stroscio and M. Dutta, *Phonons in Nanostructures* (Cambridge University Press, Cambridge, 2001).
[16] O. Madelung, *Introduction to Solid-State Theory* (Springer, Berlin, 1978).
[17] G. G. Samsonidze, R. Saito, A. Jorio, A. G. Souza Filho, A. Grüneis, M. A. Pimenta, G. Dresselhaus, and M. S. Dresselhaus, Phys. Rev. Lett. **90**, 027403 (2003).
[18] A. E. H. Love, *Treatise on the Mathematical Theory of Elasticity* (Dover, New York, 1944).
[19] J. W. S. Rayleigh, *The theory of sound* (Dover, New York, 1976).
[20] S. P. Timoshenko and S. Woinowsky-Krieger, *Theory of Plates and Shells* (McGraw-Hill, New York, 1959).
[21] S. P. Timoshenko and J. M. Gere, *Theory of Elastic Stability* (McGraw-Hill, New York, 1961).
[22] R. N. Arnold and G. B. Warburton, Proc. Roy. Soc. A **197**, 238 (1949).
[23] B. I. Yakobson, C. J. Brabec, and J. Bernholc, Phys. Rev. Lett. **76**, 2511 (1996).
[24] J. Kürti, V. Zólyomi, M. Kertesz, and G. Sun, New Journal of Physics **5**, 125.1 (2003).
[25] Y. N. Gartstein, A. A. Zakhidov, and R. H. Baughman, Phys. Rev. B **68**, 115415 (2003).
[26] D. H. Robertson, D. W. Brenner, and J. W. Mintmire, Phys. Rev. B **45**, 12592 (1992).
[27] See Appendix A for a discussion of some of these issues for a simpler example.